LONGITUDINAL AND TRANSVERSE OPTIMIZATION FOR A HIGH REPETITION RATE INJECTOR[1]

C. F. Papadopoulos, D. Filippetto, R. Huang, G. J. Portmann, H. Qian, F. Sannibale, S. Virostek, R. Wells, LBNL, Berkeley, California, USA
A. Bartnik, I. V. Bazarov, B. Dunham, C. Gulliford, C. Mayes, Cornell University (CLASSE), Ithaca, New York, USA
A. Vivoli, Fermilab, Batavia, Illinois, USA
A. Brachmann, D. Dowell, P. J. Emma, Z. Li, T. Raubenheimer, J. Schmerge, T. Vecchione, F. Zhou, SLAC, Menlo Park, California, USA

Abstract

The injector is the low energy part of a linac, where space charge and non relativistic kinematic effects may affect the electron beam quality significantly, and in the case of single pass systems determines the brightness in the downstream components. Following the increasing demand for high repetition rate user facilities, a normal conducting, high repetition rate (1 MHz) RF gun operating at 186 MHz has been constructed at LBNL and is under operation. In the current paper, we report on the status of the beam dynamics studies. For this, a multi-objected approach is used, where both the transverse and the longitudinal phase space quality is optimized, as quantified by the transverse emittance and the bunch length and energy spread respectively. We also report on different bunch charge operating modes, as well as the effect of different gun gradients.

INTRODUCTION

LCLS-II [1] is a proposed user facility based on a superconducting RF linac driving a high repetition rate FEL, at SLAC. One of the important components of the project that have been identified is the injector part, which needs to accommodate the simultaneous objectives of high repetition rate and high beam brightness. For this reason, the Advanced Photoinjector Experiment (APEX) [2], an R&D project, is under way at LBNL, and is currently the baseline for LCLS-II. APEX is based on a normal conducting, continuous wave (CW) VHF electron gun, operating at 186 MHz. Another option being investigated in parallel is a photoinjector based on DC gun technology at Cornell University [3]. In the rest of the paper, the injector beam dynamics based on the VHF gun will be presented.

LCLS-II Injector Requirements

In order to accommodate the scientific requirements of LCLS-II [1], the requirements on the electron beam at the injector exit are given in Table 1.

A number of these requirements have already been demonstrated at APEX [2], specifically the ones related to the operation of the gun only, such as quantum efficiency, bunch charge and electron energy at the gun exit.

Simulations of the APEX and LCLS-II injectors, discussed later in this paper, show that the brightness requirements can be achieved by APEX. For the experimental verification of this, the installation of APEX phase II is required, which will bring the energy of the beam higher (30 MeV) and allow for the demonstration of beam emittance, bunch compression and the conservation of 6D beam brightness.

INJECTOR LAYOUT

A schematic of the baseline design of the LCLS-II injector, based on the NCRF VHG electron gun, is shown in Fig. 1

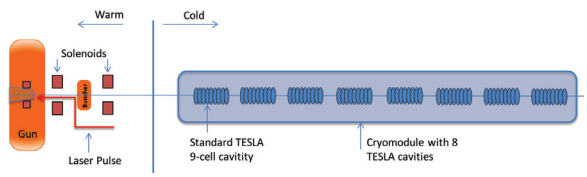

Figure 1: Schematic of LCLS-II injector. The beam energy at the warm-to-cold transition is nominally 750 keV.

The main difference with APEX is the cold part of the injector. In the case of LCLS-II, superconducting TESLA cavities [4] are used, while APEX will be using 3 normal conducting cavities, at 1.3 GHz like the TESLA ones. The final energy of APEX will be lower than 95 MeV, at approximately 30 MeV, enough to demonstrate the main dynamical processes of emittance compensation and bunch compression. The warm part of the LCLS-II injector [5] is essentially identical to the APEX layout.

As discussed below, for some bunch charges and especially the high (300 pC) case, the optimization requires relatively low gradient in the second and third TESLA cavities. This opens the possibility of having a single capture cavity in a stand-alone cryomodule followed by a drift and then a standard, 8 cavity cryomodule. Such a layout has the advantage of allowing more diagnostics as well as easing the maintenance procedure. The implications of using different layouts is discussed in a later section.

[1] This work was supported in part by the Work supported, in part, by the LCLS-II Project and by the Director of the Office of Science of the US Department of Energy under Contract no. DEAC02-05CH11231

ISBN 978-3-95450-133-5

Table 1: LCLS-II Injector Requirements

Parameter	Symbol	nominal	range	units
Electron energy at gun end	E_{gun}	750	500 - 800	keV
Electron energy at injector end	E_{inj}	98	95 - 120	MeV
Bunch Charge	Q_b	100	10 - 300	pC
Bunch Repetition Rate in Linac	f_b	0.62	0 - 0.93	MHz
Dark current in injector	I_D	0	0 - 400	nA
Peak current in injector	I_{pk}	12	4-50	A
Average current in injector	I_{avg}	0.062	0.0 - 0.3	mA
Avg. beam power at injector end	P_{av}	6.1	0 - 36	kW
Norm. rms slice emittance at injector end	$\gamma\epsilon_\perp$	0.4	0.2 - 0.6	mm
Vacuum Pressure	P_G	1	0.1 - 1	nTorr
Cathode quantum efficiency	QE	2	0.5 - 10	%
Laser Energy at cathode	E_{laser}	0.02	0.0 - 0.3	mJ
Avg. CW RF gradient (powered cavities)	E_{acc}	16	-	MV/m

OPTIMIZATION PROCEDURE

As shown in Table 1, the two main requirements on the brightness of the beam at the injector exit is the transverse emittance $\gamma\epsilon_\perp$ and the peak bunch current I_{pk}. In the case of transverse emittance, the goal is to achieve low values. The injector system described here is essentially cylindrically symmetric, which allows us to use the normalized emittance in one transverse plane ϵ_{nx} as one of the objectives to be minimized. Effects that break the symmetry, most importantly dipole and quadrupole components of the RF field in the RF cavities are beyond the scope of this paper, but are currently under evaluation. In the case of the current, I_{pk} is inverse to the bunch length σ_z for reasonably symmetric beams, and an alternative way to perform the optimization is to minimize σ_z.

Space charge at the low energy of the injector couples the longitudinal and transverse planes, and hence the two goals of minimizing the emittance and the bunch length are essentially competing. For such multi-objective, non-linearly coupled problems, the method of multi-objective genetic optimization has been applied with great success [6, 7]. In our approach, we employ the NSGA-II algorithm, with ϵ_{nx} and σ_z being the competing objectives. In this case, the result is not a single solution, but a population of solutions, a so-called Pareto front. This way, trade-offs between the two competing objectives can be evaluated easily. Also, the effect of varying certain aspects of the injector system (such as bunch charge, gun energy and injector layout) can also be evaluated visually, as will be discussed below.

In addition to these two objectives, certain constraints are also placed in the optimizer. The most obvious ones are the constraints on the knobs used in the optimizer, which are described in Table 2.

Other, secondary constraints that are placed on the beam quantities themselves are a) the total energy > 90 MeV, b) the correlated rms energy spread < 1% (in order to accommodate the energy acceptance of the laser heater) and c) the high order, correlated momentum spread $\sigma_{pHO} < \sigma_{max,Q}$,

Table 2: Knobs Used for Injector Optimization. All cavity fields refer to on-axis, peak electric field. Phase of 0 is taken to mean peak acceleration and -90 is zero crossing.

Knob	Value	Function
Gun Phase	-15-15 deg	Control bunch length
Buncher field	0-4 MV/m	Compression, Emit. comp.
Sol 1 B field	0.01-0.2 T	Emit. comp.
Sol 2 B field	0.01-0.2 T	Emit. comp.
CAV 1 field	5-30.5 MV/m (2.6 - 16 MV/m avg)	Emit. comp.
CAV 2 field	5-30.5 MV/m (2.6 - 16 MV/m avg)	Emit. comp.
RMS spot size at the cathode	0.05-2 mm	Control space charge effects
Bunch length at cathode	10-60 ps	Control space charge effects

where $\sigma_{max,Q}$ is a limit that depends on the downstream compression, which is different for different bunch charges.

The high order momentum spread is defined by the relation $\sigma^2_{pHO} = \langle p^2_{HO} \rangle$, where the momentum p_{HO} is constructed from the original momentum distribution $p(z) = p_0 + c_1 z + c_2 z^2 + O(z^3)$. The variable z refers to the longitudinal position in the bunch and p_{HO} is given by the $p_{HO} = O(z^3)$ terms. Physically, this can be justified since the p_0 term is the average momentum which doesn't affect beam brightness, and the terms corresponding to c_1 and c_2 can be removed by dephasing the downstream linac and by using a third harmonic cavity downstream respectively. Both of these are standard practices in linac driven FEL facilities. The precise value of the limit imposed on σ_{pHO} depends on the downstream linac dynamics [8, 9].

Finally, the assumption of a thermal emittance coefficient of 0.65 mm-mrad/mm is made in the following simulations.

ISBN 978-3-95450-133-5

The exact value of this coefficient will of course be determined by measurements, currently underway, and may affect the final emittance of the beam. We should note here, that due to the optimization procedure we follow, the emittance is not the minimum possible achievable by the injector, since we also need to compress the beam. Hence, the effect of the thermal emittance coefficient is reduced, as other effects such as space charge, solenoid aberrations etc, increase the emittance. In addition to this, the subsequent plots correspond to simulations with a relatively low number of macroparticles (10k) and a relatively small number of grid points (30× 50), in order to allow for a large number of solutions. This gives typically a larger number for the projected and slice emittance of the beam than finer simulations. Once a solution is picked, more accurate simulations (250k particles, 50× 100 grid points) are used for start-to-end runs.

In the next sections, the effect of varying different aspects of the injector is discussed, and simulation results based on multi-objective optimization of the injector are presented, using the particle-in-cell code ASTRA [10].

DEPENDENCE ON BUNCH CHARGE

The bunch charge is the most fundamental characteristic of the electron bunch, and determines the emittance and transverse size of the beam. Different operational modes of the downstream FEL require different bunch charges, with specs described in Table 1.

In Fig. 2 we compare different bunch charges, at 20, 100 and 300 pC. As discussed previously, the result is not a single solution, but a front of solutions. Hence, for each case we can pick a solution that meets the specs of the specific run, while at the same time we are able to easily compare the performance of different charges.

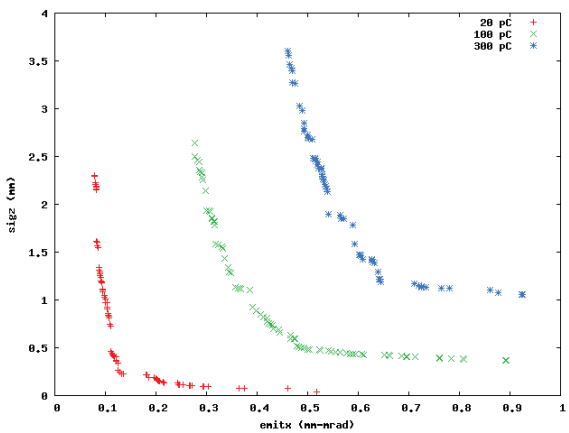

Figure 2: Comparison of Pareto fronts for different charges. Simulations for injector layout of Fig .1 at gun energy 750 keV

One important point for beam dynamics is that, especially in the case of 300 pC, the optimization algorithm sets the gradient of the 2nd and 3rd cavities to very low gradients and effectively results in a long drift between the 1st and the 4th accelerating cavities. In Fig. 3, we compare the emittance evolution for 3 of the solutions corresponding to Fig 2, with a finer grid. We see that the emittance compensation process is complete by the exit of the injector, and that a significant part of the process is done while the beam is in the 2nd and 3rd accelerating cavities, at a distance of 4-6 meters from the cathode, corresponding to energies 10-30 MeV (different for each charge optimization).

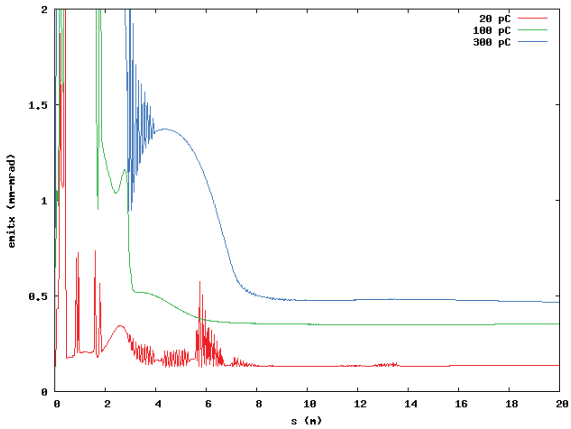

Figure 3: Comparison of emittance evolution for solutions corresponding to Fig. 2. Note that the emittance compensation is finalized at about 8 m.

EVALUATING DIFFERENT INJECTOR LAYOUTS

As mentioned in the previous section, the emittance compensation process is not finalized until after the 1st TESLA cavity in the cryomodule. This implies that it may be better to avoid accelerating the beam too quickly after the 1st cavity, in order to avoid freezing-in the emittance before the compensation process is finalized. In addition to this, a single cryomodule for the 1st cavity has other advantages, as it allows easier maintenance and additional diagnostics. For this reason, a "layout 2" case, which comprises of a single cavity cryomodule, a drift and then the standard 8 cavity cryomodule is also considered, in addition to "layout 1" shown in Fig. 1.

Beam dynamics considerations, especially for lower gun energy, may also require additional gradient and phase knobs in the first few MeV. For this reason, "layout 3" and "layout 4" are also considered, where the single cavity cryomodule is replaced by 5 2-cell cavities based on a Cornell design [3] or by 2 2-cell cavities and a standard TESLA cavity, respectively.

The different options are summarized schematically in Fig. 4.

The Pareto fronts corresponding to the layouts described are shown in Fig. 5, where we can compare the brightness performance of the different schemes, for the same gun energy.

ISBN 978-3-95450-133-5

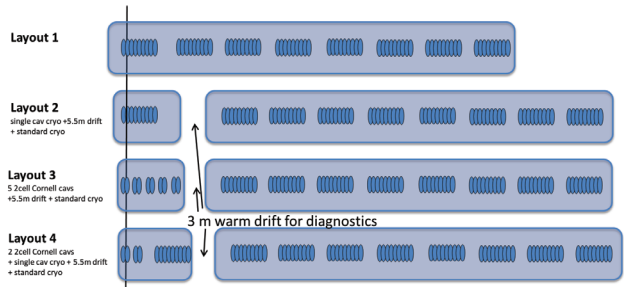

Figure 4: Different layout options for the cold part of the LCLS-II injector. Layout 1 is the baseline option.

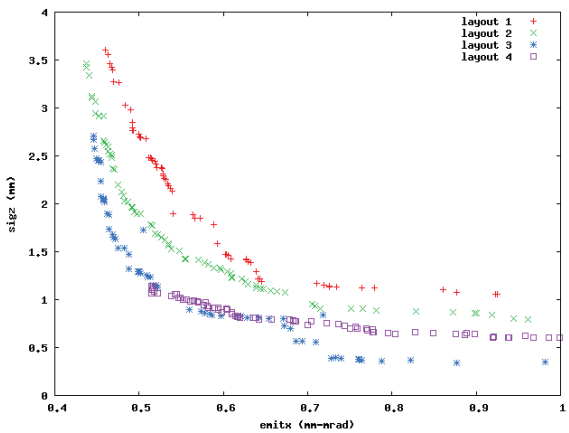

Figure 5: Comparison of Pareto fronts for different injector layouts. Gun energy is 750 keV, bunch charge 300 pC.

DEPENDENCE ON GUN ENERGY

One of the most important quantities that has a great effect on the beam brightness is the gun gradient. In general, higher gradients improve the beam quality, and in the case of the VHF gun this corresponds to higher energies at the gun exit. One potential reason to limit the gradient at the cathode is to reduce the dark current emitted from the gun, although a passive collimation system has also been proposed [11].

We should also point out that the the peak energy measured at the exit of the VHF gun is 800 keV, while the nominal, operational energy is 750 keV.

In Fig. 6, a comparison of Pareto fronts for different energies is presented, for 100 pC. The layout in this case is very similar to layout 1 discussed previously, and more studies are under way for all the layouts.

CONCLUSIONS

We report on the status of beam dynamics simulations for the LCLS-II injector. A multi-objective optimization strategy is employed, which allows the simultaneous optimization of transverse and longitudinal phase space.

By using this approach, comparisons of varying different aspects of the injector, such as bunch charge, injector layout and gun energy are presented.

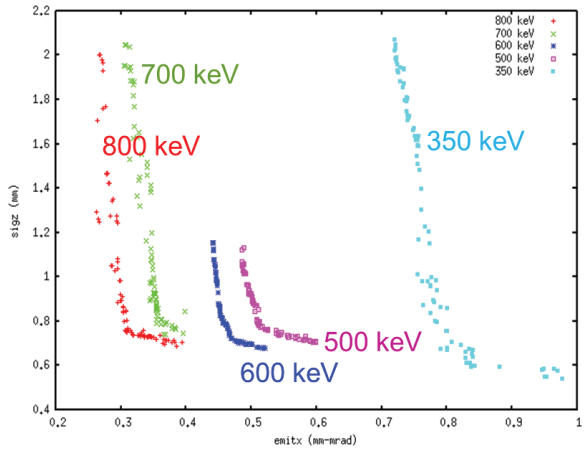

Figure 6: Comparison of Pareto fronts for different energies of the gun.

REFERENCES

[1] Tor Raubenheimer. The LCLS-II, a New FEL Facility at SLAC. In *Proc. 36th Int. Free-Electron Laser Conf., Basel, 2014*, 2014. WEB01.

[2] Daniele Filippetto et al. APEX: A Photo-injector for High Average Power Light Sources and Beyond. In *Proc. 36th Int. Free-Electron Laser Conf., Basel, 2014*, 2014. TUA01.

[3] Colwyn Gulliford et al. Demonstration of low emittance in the cornell energy recovery linac injector prototype. *Phys. Rev. ST Accel. Beams*, 16:073401, Jul 2013.

[4] B. Aune et al. Superconducting tesla cavities. *Phys. Rev. ST Accel. Beams*, 3:092001, Sep 2000.

[5] John Schmerge et al. The LCLS-II Injector Design. In *Proc. 36th Int. Free-Electron Laser Conf., Basel, 2014*, 2014. THP042.

[6] Ivan V. Bazarov and Charles K. Sinclair. Multivariate optimization of a high brightness dc gun photoinjector. *Physical Review Special Topics - Accelerators and Beams*, 8(3):034202, Mar 2005.

[7] K. Deb. *Multi-objective optimization using evolutionary algorithms*. Wiley, 2001.

[8] Lanfa Wang et al. Multi-objective Genetic Optimization for LCLS-II X-ray FEL. In *Proc. 36th Int. Free-Electron Laser Conf., Basel, 2014*, 2014. THP029.

[9] Paul Emma et al. Linear Accelerator Design for the LCLS-II FEL Facility. In *Proc. 36th Int. Free-Electron Laser Conf., Basel, 2014*, 2014. THP025.

[10] K. Flöttmann. ASTRA: A space charge tracking algorithm. *user's manual available at http://www. desy. de/~ mpyflo/Astra_dokumentation*.

[11] Ruixuan Huang et al. Dark Current Studies at the APEX Photoinjector. In *Proc. 36th Int. Free-Electron Laser Conf., Basel, 2014*, 2014. THP054.

ISBN 978-3-95450-133-5